ANALYTICAL SCIENCES MAY 2016, VOL. 32

Fluorescence Detection of DNA Based on Non-covalent π-π Stacking Interaction between 1-Pyrenebutanoic Acid and Hypericin

Weiwen HU,* Jian ZHANG,† and Jinming KONG*†**

**School of Environmental and Biological Engineering, Nanjing University of Science & Technology, Nanjing 210094, P. R. China*
***Laboratory of Translational Medicine, Jiangsu Province Academy of Traditional Chinese Medicine, Nanjing 210028, Jiangsu Province, P. R. China*

Herein, we applied hypericin (Hyp) for the detection of DNA on streptavidin-functionalized magnetic beads (SA-MB) through non-covalent π-π stacking interaction between 1-pyrenebutanoic acid (PBA) and Hyp. Briefly, the target DNA (tDNA) was hybridized to morpholino oligonucleotide (MO) that was immobilized on the surface of SA-MB. PBA was incorporated to the backbone of tDNA by means of phosphate-zirconium-carboxylate coordination reaction. Then, fluorescent Hyp was linked to PBA *via* π-π stacking interaction. Under the optimal conditions, this biosensor displayed a good linear relationship between the fluorescence intensity and the tDNA concentrations in the range from 1 to 100 nM with a low detection limit of 2.9 nM. The mismatch type in a specific DNA sequence can also be efficiently discriminated. Compared with some other reports, this method is more convenient, and has great potential for practical applications.

Keywords Biosensor, magnetic beads, morpholino oligonucleotide, zirconyl chloride, 1-pyrenebutanoic acid, hypericin

(Received October 13, 2015; Accepted December 28, 2015; Published May 10, 2016)

Introduction

Hypericin (Hyp) is a natural photosensitizing agent that can be isolated from the plant *Hypericum*.[1] In previous studies, it has been used for a long time as a non-porphyrin necrosis-avid agent because of its special affinity for nonviable tissues.[2] Recently, more interest is given to some other important pharmaceutical potentials, such as antiviral, antibacterial, antitumor activities.[3-6] In addition, Hyp reveals significant potentials as an imaging marker for early assessment of the therapeutic response after percutaneous radiofrequency ablation and ethanol injection.[7,8] Most of the clinical features of Hyp are related to its low systemic toxicity, high tumor selectivity, clearance rate and phototoxicity.[9] Interaction of the excited Hyp with surrounding molecules results in two types of photo-oxidative reactions, which can both take place in the photoactivation of Hyp. One of the reactions involves electron or hydrogen atom transfer, leading to the radical form of the photosensitizer, which can react with oxygen to form reactive oxygen species, such as peroxides, superoxide and hydroxyl radicals. Another mechanism is mediated by the energy transfer directly to oxygen and the generation of its singlet form which results in apoptosis and plays a central role in the photocytotoxicity of Hyp.[10]

Hyp is readily dissolved, and remains in its monomeric form in polar organic solvents, such as dimethylsulfoxide (DMSO), ethanol, acetone and ethyl acetate. It is sparingly soluble in nonpolar organic solvents and oil. With a nearly planar conformation, Hyp is almost insoluble and forms nonfluorescent aggregates in an aqueous environment, which significantly hinders its photodynamic activity.[11-13] The photosensitizing effect of Hyp was described as singlet oxygen production when it is in organic solvent or bound to liposomic media.[14] When Hyp is aggregated in an aqueous solution, the main form of the generated active oxygen is superoxide.[15,16] In addition, the aggregation strongly depends on the pH. Hyp molecules are neutral in acidic environments, and are predominantly monoanions in a neutral environment. However, Hyp is partially soluble, and appears as a dianion in alkaline aqueous solutions. Only the neutral and monoanionic forms of Hyp tend to self-associate.[17] Hyp aggregation can have a considerable effect on the biological activity of this drug. Most of the photodynamic properties are lost upon Hyp aggregation.[18] The diffusion of Hyp aggregates in an aqueous environment may be the driving force of Hyp transport *in vivo*, which is highly important for biological and medical applications.[13,19]

In view of the fact that Hyp was in a polycyclic aromatic structure and highly fluorescent in polar organic solvents, we thought that Hyp might hold promise for molecular recognition through non-covalent π-π stacking interaction, which has never been investigated for this purpose. The π-π interaction is a very important noncovalent intermolecular force, similar to hydrogen bonding. It can contribute to the self-assembly or molecular recognition when extended structures are formed from building blocks with aromatic moieties.[20,21] The π-π interaction ranges from large biological systems to relatively small molecules,[22,23]

† To whom correspondence should be addressed.
E-mail: j.kong@njust.edu.cn; cpu-yzq@cpu.edu.cn

Table 1 MO and DNA sequences

MO	5′-AAC CAT ACA ACC TAC TAC CTC A-Biotin-3′
tDNA	5′-TGA GGT AGT AGG TTG TAT GGT T-3′
Single-base mismatched (SBM)	5′-TGA GGT AGT AGG TTG TGT GGT T-3′
Three-base mismatched (TBM)	5′-TGA GGT ATT AGA TTG TGT GGT T-3′
Non-complementary (Control)	5′-ACT TAC CTT TGC TCA TTG ACG A-3′

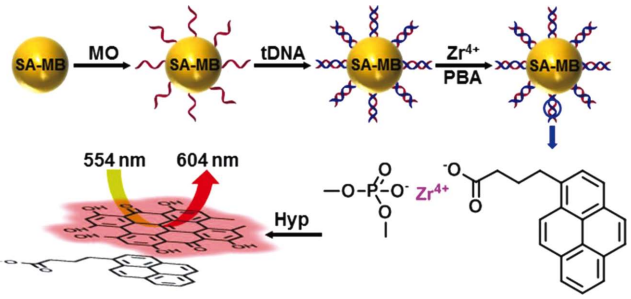

Fig. 1 Schematic diagram of this DNA sensing strategy.

which plays a significant role in the binding and conformation all the way from benzene to nucleic acid and protein.[24-26] It has been reported that the energy of a typical π-π stacking interaction is about 2 kJ/mol.[27] Based on these results, we can incorporate Hyp to another polyaromatic hydrocarbon, such as 1-pyrenebutanoic acid (PBA), which has been linked to the backbone of DNA for DNA detection.

Zirconium ions are commonly used as simple and effective linkers for various applications because they are able to bind with free phosphate groups or carboxyl groups by means of carboxylate-zirconium-phosphate coordination.[28,29] PBA, which contains a terminal carboxyl, can be strongly conjugated with the deoxyribose phosphate backbone of DNA in the presence of zirconium ions.[30,31] In this work, for the first time we applied Hyp for the detection of DNA on streptavidin-functionalized magnetic beads (SA-MB) through non-covalent π-π stacking interaction between PBA and Hyp. Herein, tDNA was hybridized to MO that was immobilized on the surface of SA-MB. MO is a nucleic acid analogue comprised of non-ionic phosphorodiamidates, morpholino rings and nucleic acid bases. It has received considerable attention as a result of its advantageous characteristics, including water solubility, resistance to enzymatic degradation, high hybridization affinity and specificity for DNA.[32] PBA was incorporated to the backbone of tDNA, and then fluorescent Hyp was linked to PBA *via* π-π stacking interaction. We ensured that the fluorescence was observed only when tDNA hybridized to the MO, because the only sites for the incorporation of PBA were the phosphates on the tDNA backbones. The water content greatly influenced Hyp incorporation because Hyp formed nonsoluble aggregates in an aqueous environment. Under the optimal conditions, this biosensor displayed a good linear relationship between the fluorescence intensity and the tDNA concentrations, with a two-orders-of-magnitude dynamic range and a low nM LOD. In addition, the single nucleotide mismatches greatly influence the hybridization efficiency. Thus, the mismatch type in a specific DNA sequence can be efficiently discriminated. Because of these intriguing properties, increasing attention will be paid to this novel application of Hyp.

Materials and Methods

Chemicals

Streptavidin-functionalized magnetic beads (diameter 100 nm) were purchased from Seebio Biotech Inc. (Shanghai, China) in a 10 mg/mL suspension. Morpholino oligonucleotide was obtained from Gene Tools LLC (Philomath, OR). DNA was synthesized by Invitrogen Biotechnology Co., Ltd. (Shanghai, China). Sequences of DNA used in this study are listed in Table 1. All of the other chemicals were purchased from Sigma-Aldrich (St. Louis, MO) without further purification. Different buffer solutions were used throughout the present work: PBS (0.1 M, pH 7.4), ×TE buffer (pH 8.0). Ultrapure water was prepared through a Millipore Milli-Q water-purification system (≥ 18.25 MΩ).

SA-MB functionalization and Hyp labeling

SA-MB were used as substrates for the immobilization of 3′ biotinylated MO due to many advantages of such small particles, including high reactivity, high dispersion, easy separation, large contact surface and functionalized surface densities.[33] Prior to the conjugation of MO with SA-MB, 2 μL of SA-MB was first magnetically separated, washed with PBS, and resuspended in 20 μL of 1 μM MO (dissolved in PBS). The mixture was incubated for 1 h with gentle shaking. The functionalized microspheres were then washed with PBS and resuspended in 20 μL of tDNA (dissolved in TE buffer). The hybridization reaction was carried out for 1 h at 37°C under gentle shaking. After hybridization, the microspheres were washed with Tris–HCl to remove any residual tDNA, and resuspended in 20 μL of 4 mM Zr^{4+} (dissolved in 60% ethanol). The mixture was incubated for 30 min with gentle shaking. Then, the microspheres were washed with 60% ethanol and resuspended in 20 μL of 2 mM PBA (dissolved in *N*,*N*-dimethylformamide, DMF). The reaction was carried out for 30 min under gentle shaking. After washing with DMF, the microspheres were resuspended in 20 μL of 0.2 mM Hyp (dissolved in DMSO) for non-covalent π-π stacking. Highly fluorescent Hyp was stably incorporated to the backbone of tDNA, as judged by UV-vis spectroscopy and fluorescence spectroscopy. The procedures for entire DNA sensing are illustrated in Fig. 1.

UV-visible absorbance and fluorescence measurements

UV-visible absorbance spectra were measured on an UV-3600 UV-VIS-NIR spectrophotometer (Shimadzu, Japan) with a sample volume of 3 mL. Fluorescence spectra were acquired on an Edinburgh FLS920 fluorescence spectrophotometer with a sample volume of 100 μL. Excitation and emission slits were all set for a 3-nm band-pass. The excitation wavelength was set at 554 nm and the emission spectra from 570 to 750 nm were recorded.

Results and Discussion

Response characteristics of this DNA sensing approach

Hyp was incorporated to the backbone of tDNA by means of phosphate-zirconium-carboxylate coordination and the π-π stacking interaction. As shown in Fig. 2b, the incorporated Hyp emitted fluorescence at around 604 nm under excitation with

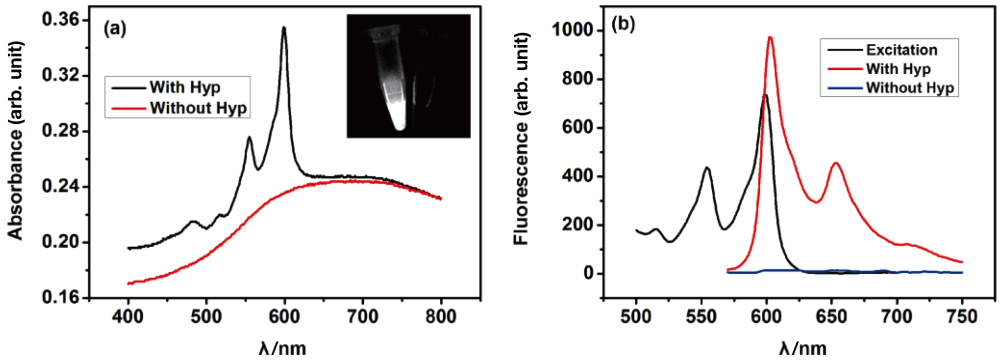

Fig. 2 UV-vis absorbance spectra with and without Hyp (a), excitation, emission (λ_{ex} = 554 nm) spectra with and without Hyp (b). Insets: photographs with (left) and without (right) tDNA under 554 nm excitation. Concentration of tDNA, 100 nM.

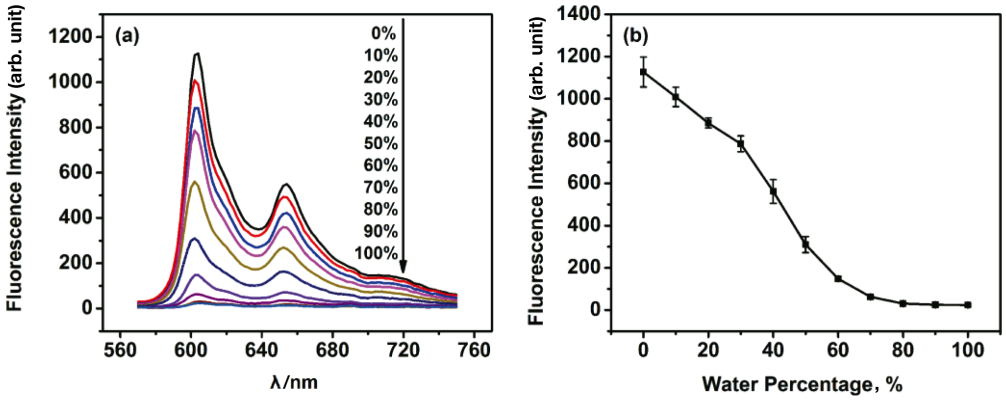

Fig. 3 Fluorescence emission spectra under different contents of water (a); change of the fluorescence intensity at λ_{em} = 604 nm (λ_{ex} = 554 nm) (b). Concentration of tDNA, 100 nM.

554 nm UV light. The characteristic absorption peak appeared in the recorded UV-vis absorption spectrum is similar to the excitation spectrum (Fig. 2a). If the tDNA was not hybridized to MO or Hyp was not incorporated, the fluorescence was practically not observed. It can be concluded that Hyp was successfully incorporated to the backbone of tDNA.

Influence of Hyp self-aggregation

With a nearly planar conformation, Hyp is almost insoluble, and forms nonfluorescent aggregates in an aqueous environment, which significantly hinders its photodynamic activity. Hyp molecules are neutral in acidic environments, and are predominantly monoanions in a neutral environment. The neutral and monoanionic forms of Hyp tend to self-associate. Two different mechanisms for neutral or monoanionic Hyp self-aggregation have been proposed so far. (1) The formation of planar aggregates through intermolecular hydrogen bonding between carbonyl and hydroxyl groups of different molecules. This aggregation form was suggested by Sevenants and further corroborated by Yamazaki.[34,35] In this model, a hydrogen-bonded planar oligomeric structure involves additional stacking of Hyp molecules. (2) Stacked aggregates of Hyp dissolved in DMSO/water mixtures were confirmed by Falk and Meyer.[36] This stacking is due to the hydrophobic effect of the aromatic core in Hyp molecules. The neighboring molecules within the stacking are rotated against each other by about 180°. Herein, the influence of the water content in the π-π stacking interaction was investigated. As shown in Fig. 3, the fluorescence decreased with the water content increasing, which can be ascribed to the self-aggregation of Hyp. A steric hindrance influenced the π-π stacking interaction between PBA and Hyp. Consequently, a polar organic solvent, such as DMSO, was necessary for the reaction of PBA with Hyp, as well as the measurement of the UV absorbance and fluorescence spectra.

Optimization of non-covalent π-π stacking time

The π-π stacking time greatly influenced the resulting fluorescence, and thus it should be carefully optimized. Herein, we fixed the tDNA concentration at 100 nM, and varied the π-π stacking time from 10 to 80 min. As shown in Fig. 4a, the fluorescence intensity increased with the π-π stacking time increasing from 10 to 50 min, and reached a plateau. Figure 4b outlines the relationship between the fluorescence intensity at λ_{em} = 604 nm (λ_{ex} = 554 nm) and the π-π stacking time. Taking these results into account, the optimal π-π stacking time was 50 min, which was adopted in following experiments.

Analytical performance of this DNA sensing approach

The analytical performance of this method was evaluated. As shown in Fig. 5, the fluorescence intensity increased with the increase of the tDNA concentration over a range from 1 to 100 nM. The calibration curve showed a good linear relationship between the fluorescence intensity at λ_{em} = 604 nm and the concentration of tDNA. The linear regression equation is

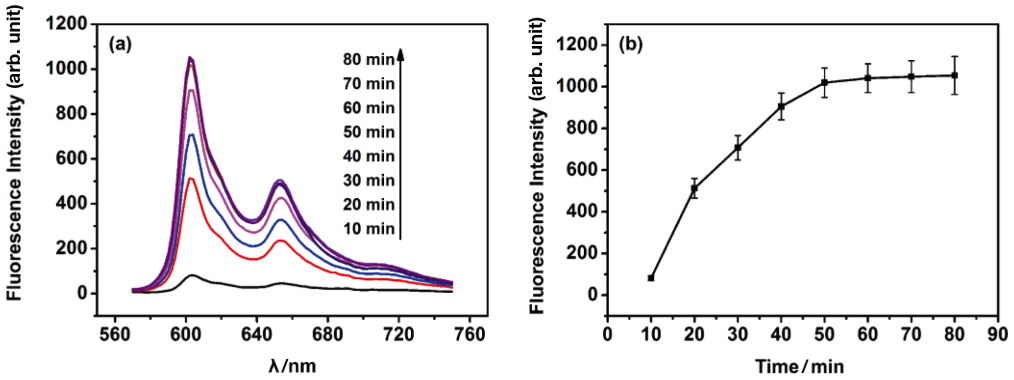

Fig. 4 Fluorescence emission spectra with different π-π stacking time (a); reaction time dependence of the fluorescence intensity at λ_{em} = 604 nm (λ_{ex} = 554 nm) (b). Concentration of tDNA, 100 nM.

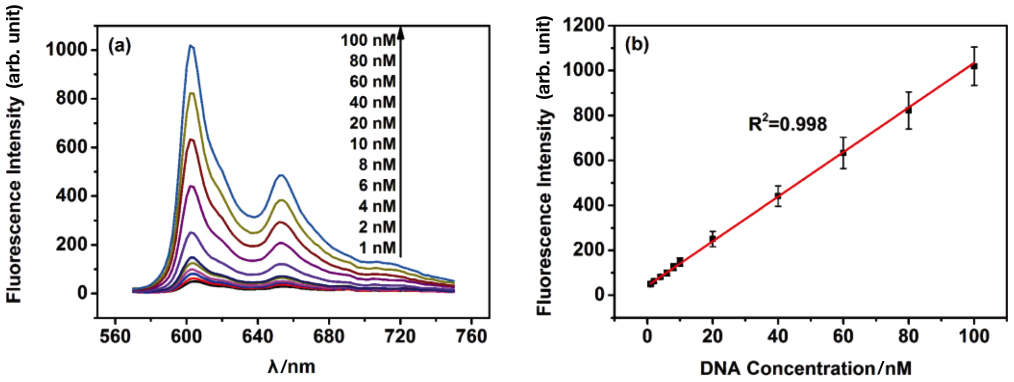

Fig. 5 Fluorescence emission spectra (λ_{ex} = 554 nm) with different concentrations of tDNA (a); fluorescence intensity at λ_{em} = 604 nm (b).

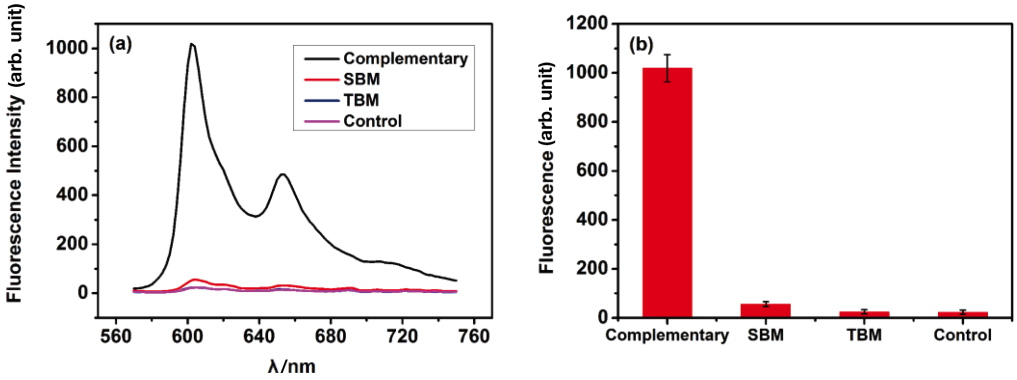

Fig. 6 Fluorescence emission spectra (λ_{ex} = 554 nm) with 100 nM DNA of different sequences (a); fluorescence intensity at λ_{em} = 604 nm (b).

$y = 9.9196x + 42.2114$ (x is the tDNA concentration (nM), y is the fluorescence intensity at λ_{em} = 604 nm, $R^2 = 0.998$). The LOD was calculated to be ~2.9 nM (S/N = 3), which is higher than some recently reported DNA fluorescent sensors, such as a linear molecular beacon based on DNA scaffolded silver nanocluster (3.2 nM),[37] assembly-line manipulation of droplets in microfluidic platform (14 nM),[38] DNA-templated silver nanoclusters (25 nM),[39] *etc.* Although the LOD is not superior to some other methods, such as a single-layer transition metal dichalcogenide nanosheet (0.05 nM),[40] WS_2 nanosheet-based platform (0.5 nM),[41] SnO_2 nanopillars (2 nM),[42] as well as our report before (98.2 pM),[43] this method is more convenient. Overall, the analytical performance of this method is quite acceptable.

The selectivity of this method was investigated by comparing the resulting fluorescence of 100 nM tDNA, SBM, TBM and control DNA. As shown in Fig. 6, the fluorescence from SBM and TBM was only 5.54 and 2.39%, respectively, of the value obtained from tDNA, indicating that this method was highly selective toward even a single base mismatch in the full

sequence. The excellent selectivity can be attributed to the difference of the hybridization efficiency between MO and DNA. The tDNA could effectively hybridize with MO for Hyp labeling, while the other sequences could not. Such results highlighted that this method could effectively discriminate mismatched sequences, and shows great potential for genotyping of single nucleotide polymorphism.

Conclusions

In summary, we for the first time applied Hyp for the detection of DNA on SA-MB through non-covalent π-π stacking interaction between PBA and Hyp. The procedures for SA-MB functionalization and Hyp labeling were described. The results clearly show that Hyp can be efficiently incorporated to the backbone of tDNA through phosphate-zirconium-carboxylate coordination and non-covalent π-π stacking interaction. The water content greatly influenced Hyp incorporation due to that Hyp formed nonsoluble aggregates in an aqueous environment. Under the optimal conditions, this biosensor displayed a good linear relationship between the fluorescence intensity and the tDNA concentrations in the range from 1 to 100 nM with a low detection limit of 2.9 nM. The mismatch type in a specific DNA sequence can also be efficiently discriminated. Compared with some other reports, this method is more convenient and has great potential for practical applications.

Acknowledgements

We are grateful to National Natural Science funding (No. 21575066) for this project and the Technology Foundation for Selected Overseas Scholar in Nanjing.

References

1. H. Falk, *Angew. Chem. Int. Ed.*, **1999**, *38*, 3116.
2. C. Jiang, Y. Li, X. Jiang, N. Yao, M. Gao, X. Zhang, J. Wang, X. Wang, Z. Sun, J. Zhang, and Y. Ni, *Photochem. Photobiol.*, **2014**, *90*, 867.
3. P. Miskovsky, *Curr. Drug Targets*, **2002**, *3*, 55.
4. M. A. D'Hallewin, A. R. Kamuhabwa, T. Roskams, P. A. M. De Witte, and L. Baert, *BJU Int.*, **2002**, *89*, 760.
5. Y. Ji, C. Jiang, X. Zhang, W. Liu, M. Gao, Y. Li, J. Wang, Q. Wang, Z. Sun, X. Jiang, N. Yao, X. Wang, Z. Fang. Z. Yin, Y. Ni, and J. Zhang, *Oncotarget*, **2014**, *5*, 2934.
6. A. Kubin, P. Meissner, F. Wierrani, U. Burner, A. Bodenteich, A. Pytel, and N. Schmeller, *Photochem. Photobiol.*, **2008**, *84*, 1560.
7. M. Van de Putte, H. Wang, F. Chen, P. A. de Witte, and Y. Ni, *Oncol. Rep.*, **2008**, *19*, 927.
8. M. Van de Putte, H. Wang, F. Chen, P. A. de Witte, and Y. Ni, *Acad. Radiol.*, **2008**, *15*, 107.
9. H. R. Vardapetyan, A. S. Martirosyan, S. G. Tiratsuyan, and A. A. Hovhannisyan, *J. Photochem. Photobiol. B*, **2010**, *101*, 53.
10. P. Agostinis, A. Vantieghem, W. Merlevede, and P. A. de Witte, *Int. J. Biochem. Cell Biol.*, **2002**, *34*, 221.
11. S. M. Arabei, T. A. Pavich, J. P. Galaup, and P. Jardon, *Chem. Phys. Lett.*, **1999**, *306*, 303.
12. S. Kascakova, M. Refreglers, D. Jancura, F. Sureau, J. C. Maurizot, and P. Miskovsky, *Photochem. Photobiol.*, **2005**, *81*, 1395.
13. G. Bánó, J. Staničová, D. Jancura, J. Marek, M. Bánó, J. Uličný, and P. Miškovský, *J. Phys. Chem. B*, **2011**, *115*, 2417.
14. A. P. Darmanyan, L. Burel, D. Eloy, and P. Jardon, *J. Chim. Phys.*, **1994**, *91*, 1774.
15. L. Weiner and Y. Mazur, *J. Chem. Soc. Perkin Trans.*, **1992**, *2*, 1439.
16. T. Youssef, *Photochem. Photobiol.*, **2009**, *85*, 921.
17. E. I. Kapinus, H. Falk, and H. T. Tran, *Monatsh. Chem.*, **1999**, *130*, 623.
18. G. Lajos, D. Jancura, P. Miskovsky, J. V. Garcia-Ramos, and S. Sanchez-Cortes, *J. Phys. Chem. C*, **2008**, *112*, 12974.
19. M. Van De Putte, T. Roskams, G. Bormans, A. Verbruggen, and P. A. De Witte, *Int J. Oncol.*, **2006**, *28*, 655.
20. D. B. Amabilino and J. F. Stoddart, *Chem. Rev.*, **1995**, *95*, 2725.
21. C. Janiak, *J. Chem. Soc. Dalton Trans.*, **2000**, *21*, 3885.
22. C. A. Hunter, *Chem. Soc. Rev.*, **1994**, *23*, 101.
23. S. P. Brown, I. Schnell, J. D. Brand, K. Müllen, and H. W. Spiess, *J. Am. Chem. Soc.*, **1999**, *121*, 6712.
24. C. A. Hunter, J. Singh, and J. M. Thornton, *J. Mol. Biol.*, **1991**, *218*, 837.
25. K. M. Guckian, B. A. Schweitzer, R. X. F. Ren, C. J. Sheils, D. C. Tahmassebi, and E. T. Kool, *J. Am. Chem. Soc.*, **2000**, *122*, 2213.
26. K. Müller-Dethlefs and P. Hobza, *Chem. Rev.*, **2000**, *100*, 143.
27. W. L. Jorgensen and D. L. Severance, *J. Am. Chem. Soc.*, **1990**, *112*, 4768.
28. I. O. Benítez, B. Bujoli, L. J. Camus, C. M. Lee, F. Odobel, and D. R. Talham, *J. Am. Chem. Soc.*, **2002**, *124*, 4363.
29. G. Nonglaton, I. O. Benitez, I. Guisle, M. Pipelier, J. Léger, D. Dubreuil, C. Tellier, D. R. Talham, and B. Bujoli, *J. Am. Chem. Soc.*, **2004**, *126*, 1497.
30. R. J. Chen, Y. Zhang, D. Wang, and H. Dai, *J. Am. Chem. Soc.*, **2001**, *123*, 3838.
31. Y. L. Zhao and J. F. Stoddart, *Accounts Chem. Res.*, **2009**, *42*, 1161.
32. J. Summerton and D. Weller, *Antisense Nucleic Acid Drug Dev.*, **1997**, *7*, 187.
33. A. H. Lu, E. L. Salabas, and F. Schüth, *Angew. Chem.*, **2007**, *46*, 1222.
34. M. R. Sevenants, *J. Protozool.*, **1965**, *12*, 240.
35. T. Yamazaki, N. Ohta, I. Yamazaki, and P. S. Song, *J. Phys. Chem.*, **1993**, *97*, 7870.
36. H. Falk, J. Meyer, and M. Oberreiter, *Monatsh. Chem.*, **1993**, *124*, 339.
37. J. L. Ma, B. C. Yin, and B. C. Ye, *RSC Adv.*, **2015**, *5*, 65437.
38. J. Chen, G. Zhou, Y. Liu, T. Ye, X. Xiang, X. Ji, and Z. He, *Talanta*, **2015**, *134*, 271.
39. Y. Zhang, C. Zhu, L. Zhang, C. Tan, J. Yang, B. Chen, L. Wang, and H. Zhang, *Small*, **2015**, *11*, 1385.
40. Y. Zhang, B. Zheng, C. Zhu, X. Zhang, C. Tan, H. Li, B. Chen, J. Yang, J. Chen, Y. Huang, L. Wang, and H. Zhang, *Adv. Mater.*, **2015**, *27*, 935.
41. S. Wang, Y. Zhang, Y. Ning, and G. J. Zhang, *Analyst*, **2015**, *140*, 434.
42. M. H. Le, L. Fradetal, D. Delabouglise, A. T. Mai, and V. Stambouli, *Electroanalysis*, **2015**, *27*, 1210.
43. W. Hu, Y. Ning, J. Kong, and X. Zhang, *Analyst*, **2015**, *140*, 5678.